

## Structural, Magnetic and Electrical Properties of Barium Titanate and Magnesium Ferrite Composites

(Struktur, Sifat Magnet dan Elektrik Komposit Barium Titanat dan Ferit Magnesium)

MOHAMAD FAHMI AMIN BIN ZOLKEPLI & ZALITA ZAINUDDIN\*

### ABSTRACT

*Structural, magnetic and electrical characteristics of multiferroics  $(1-x)\text{BaTiO}_3-x\text{MgFe}_2\text{O}_4$  composites with weight fractions of  $x = 0.3, 0.5$  and  $0.7$  are reported.  $\text{MgFe}_2\text{O}_4$  powders were prepared using sol-gel auto combustion technique. It was combined with commercial  $\text{BaTiO}_3$  to form composites by using wet milling solid state reaction technique. Formation of tetragonal perovskite for the ferroelectric  $\text{BaTiO}_3$  and cubic spinel for the ferrimagnetic  $\text{MgFe}_2\text{O}_4$  phases, were identified from the XRD pattern. The average grain size for each composite was about  $0.5 \mu\text{m}$ . The M-H loop showed soft ferrimagnetic properties due to the presence of  $\text{MgFe}_2\text{O}_4$  in the composites. The increment of the  $\text{MgFe}_2\text{O}_4$  weight fraction increased the saturation magnetization and slightly changed the coercive field. The complex impedance plot can be represented by a parallel R and C circuit. Composite sample with  $x = 0.5$  has the highest resistance with lowest capacitance and dielectric constant value at room temperature. The dielectric constant showed a very strong dispersion at low frequencies, due to the Maxwell-Wagner mechanism and a slight dispersion at higher frequencies. Based on the results obtained, all of the composite samples exhibited high dielectric constant and tangent loss at the low frequency range.*

*Keyword: Ceramic; dielectric; ferrimagnet; ferroelectric*

### ABSTRAK

*Struktur, sifat magnet dan elektrik komposit multiferroik  $(1-x)\text{BaTiO}_3-x\text{MgFe}_2\text{O}_4$  dengan pecahan berat,  $x = 0.3, 0.5$  dan  $0.7$  dilaporkan. Serbuk  $\text{MgFe}_2\text{O}_4$  telah disediakan menggunakan teknik sol-gel pembakaran auto. Ia digabungkan bersama  $\text{BaTiO}_3$  komersil untuk membentuk komposit dengan menggunakan teknik tindak balas keadaan pepejal pengisaran basah. Pembentukan fasa perovskit tetragon bagi feroelektrik  $\text{BaTiO}_3$  dan fasa kubus spinel bagi ferimagnet  $\text{MgFe}_2\text{O}_4$ , dikenal pasti daripada corak XRD. Purata saiz butiran setiap komposit ialah  $0.5 \mu\text{m}$ . Lengkung M-H menunjukkan sifat-sifat ferimagnet lembut disebabkan oleh kehadiran  $\text{MgFe}_2\text{O}_4$  di dalam komposit. Kenaikan pecahan berat  $\text{MgFe}_2\text{O}_4$  meningkatkan pemagnetan tepu dan mengubah sedikit medan paksa. Plot impedans kompleks boleh diwakili oleh litar selari R dan C. Sampel komposit  $x = 0.5$  mempunyai rintangan tertinggi serta nilai kapasitans dan pemalar dielektrik terendah pada suhu bilik. Pemalar dielektrik menunjukkan penyerakan yang tinggi pada frekuensi rendah disebabkan mekanisme Maxwell-Wagner dan sedikit penyerakan pada frekuensi lebih tinggi. Berdasarkan hasil yang diperolehi, kesemua sampel komposit memaparkan pemalar dielektrik dan kehilangan tangen yang tinggi pada julat frekuensi rendah.*

*Kata kunci: Dielektrik; ferimagnet; feroelektrik; seramik*

### INTRODUCTION

A wide range of multiferroics materials have been studied due to their special properties and technological applications (Spaldin et al. 2010). This type of material has more than one ferroics ordering such as ferroelectricity and ferromagnetic ordering where the electrical polarization can be switched with magnetization switching and vice versa (Roy et al. 2012). Ferroelasticity and ferrotoroidics are two other ferroics ordering that may exist in the multiferroics materials. Multiferroics materials may exist as single phase or as composites form (Zolkepli & Zainuddin 2015). Single phase multiferroics are materials that have simultaneous interaction between two or more primary ferroics order. However, due to lack of single phase materials, multiferroics in composite form are being considered

(Fina et al. 2010). Significant interest in the multiferroics composite research due to their multifunctionality leads to the combination between ferroelectric and piezoelectric material with the magnetic material.  $\text{BaTiO}_3\text{-CoFe}_2\text{O}_4$ ,  $\text{NiFe}_2\text{O}_4\text{-BaTiO}_3$  and  $\text{BaTiO}_3\text{-Ni}_{0.7}\text{Zn}_{0.3}\text{Fe}_2\text{O}_4$  are examples of some multiferroics composites with combination of ferrimagnetic and ferroelectric materials (Leonel et al. 2011; Liu et al. 2013; Zhang et al. 2013). The ferrimagnet-ferroelectric characteristic can be used in multifunctional devices such as sensors, actuators and magnetoelectric transducers.

Spinel ferrite, such as  $\text{MgFe}_2\text{O}_4$  and  $\text{CoFe}_2\text{O}_4$ , consists of two crystallographic sites which are the tetragonal and octahedral sites. The oxygen atoms forms an arrangement of cubic closed-packed (Sutka & Mezinskis 2012). Spinel

ferrite has been used for magnetic switches, magnetic resonance imaging, drug delivery, magnetic ferrofluids, high-density data storage, microwave absorber and magnetic bulk cores (Yadav et al. 2016). Besides that, spinel ferrite was used in medicine because it is not damaging the tissues and magnetic properties remains unchanged after medical used (Siong et al. 2013). Ferrite was also hybridized with carbon nanotube to improve its magnetic properties and its dielectric properties (Yu et al. 2012). Meanwhile,  $\text{BaTiO}_3$  was widely studied due to its wide application and various properties of ferroelectric, piezoelectric and dielectric. It becomes an option to be used in applications such as multilayer capacitors, thermistors and electrooptic devices.  $\text{BaTiO}_3$  also has high dielectric constant and low tangent loss. Curie temperature of  $\text{BaTiO}_3$  is about  $120^\circ\text{C}$  where at this temperature, it undergoes a phase transition from tetragonal to cubic and loss its ferroelectric properties. Research on the coupling between fine grained  $\text{BaTiO}_3$ - $\text{MgFe}_2\text{O}_4$  composite prepared using Pechini-like method has been conducted by Köferstein et al. (2015).

Based on previous research, different compositions of perovskite  $\text{BaTiO}_3$  and spinel ferrite powders altered the electrical and magnetic properties of the composite (Liu et al. 2013; Ravindar Tadi et al. 2010). In this study,  $\text{MgFe}_2\text{O}_4$  powders were synthesized via the sol-gel autocombustion method and then combined with commercial  $\text{BaTiO}_3$  powders at 3 different weight fractions through a simple wet milling solid state reaction process to obtain  $\text{BaTiO}_3$ - $\text{MgFe}_2\text{O}_4$  composite materials with potential multiferroics properties. We will discuss on how variation of weight fractions of the composites could affect the structure, magnetic and electrical properties of the materials.

#### MATERIALS AND METHODS

$(1-x)\text{BaTiO}_3$ - $x\text{MgFe}_2\text{O}_4$  composite samples with different weight fraction of  $x = 0.3, 0.5$  and  $0.7$  were prepared using the wet ball milling process.  $\text{BaTiO}_3$  powders were obtained commercially (Sigma Aldrich  $< 2 \mu\text{m}$ , 99.9%), whereas  $\text{MgFe}_2\text{O}_4$  powders had been synthesized using the sol-gel auto combustion technique. Starting materials that have been used for the  $\text{MgFe}_2\text{O}_4$  preparation were iron (III) nitrate nonahydrate  $\text{Fe}(\text{NO}_3)_3 \cdot 9\text{H}_2\text{O}$  (Sigma Aldrich, 98%), magnesium nitrate hexahydrate  $\text{Mg}(\text{NO}_3)_2 \cdot 6\text{H}_2\text{O}$  (Sigma Aldrich, 99%) and citric acid monohydrate  $\text{C}_6\text{H}_8\text{O}_7 \cdot \text{H}_2\text{O}$  (Merck KGaA, 99.95%). The molar ratio of citric acid monohydrate to metal nitrate was fixed at 1:2. Each starting materials were mixed, dissolved and stirred in deionized water until they are completely dissolved. Next, ammonia solution was dropped until the pH value of the solution approached 7. The solution was stirred and heated at  $95^\circ\text{C}$  until the solution slowly evaporated to form brown gel. The dehydration process was continued until the gel turned into a fluffy mass and burnt in an autocombustion manner. After that, the  $\text{MgFe}_2\text{O}_4$  precursor was grinded to get fine  $\text{MgFe}_2\text{O}_4$  powders.

Both  $\text{BaTiO}_3$  and  $\text{MgFe}_2\text{O}_4$  powders were then weighted according to the predetermined percentage and milled in ethanol using agate balls at 250 rpm for 5 h. The slurry was then dried at  $100^\circ\text{C}$  for an hour and subsequently grinded. The dried powders then uniaxially pressed by applying pressure of 147 MPa to form a 13 mm diameter pellet, which was finally sintered in air at  $1100^\circ\text{C}$  for 3 h.

Structural and phases determination of the composites powders were performed at room temperature using an X-ray diffractometer, model D8 Advance Bruker AXS Germany with  $\text{CuK}\alpha$  ( $\lambda = 0.15406 \text{ nm}$ ) up to  $2\theta$  of  $90^\circ$  with a scanning speed  $0.025^\circ/\text{step}$  and under 40 kV and 40 mA condition. The morphology and microstructure of the composites fractured pellets were observed by using the field-emission scanning microscope (FESEM, Supra 55VP). Magnetic hysteresis loop was investigated using Vibrating Sample Magnetometer (VSM, LakeShore/7404). Circular platinum electrodes were sprayed on both sintered pellet surfaces and electrically analyzed by Solartron 1260 Impedance/gain-phase analyzer.

#### RESULTS AND DISCUSSION

X-ray diffraction patterns of the  $(1-x)\text{BaTiO}_3$ - $x\text{MgFe}_2\text{O}_4$  composites with different weight fractions of  $x = 0.3, 0.5$  and  $0.7$  are shown in Figure 1. The peaks of XRD pattern were indexed and matched with the JCPDS 01-070-9164 and JCPDS00-017-0464 for tetragonal perovskite  $\text{BaTiO}_3$  and cubic spinel  $\text{MgFe}_2\text{O}_4$  phases, respectively. The relative peak intensity of  $\text{MgFe}_2\text{O}_4$  phase increases when its weight fraction increases, while the  $\text{BaTiO}_3$  peaks decrease as expected. The results also showed no formation of new phases, which indicates the chemical reaction between  $\text{BaTiO}_3$  and  $\text{MgFe}_2\text{O}_4$  did not happen during milling and sintering process. This was further confirmed using *TOPAS*, which is a new generation profile and structure analysis

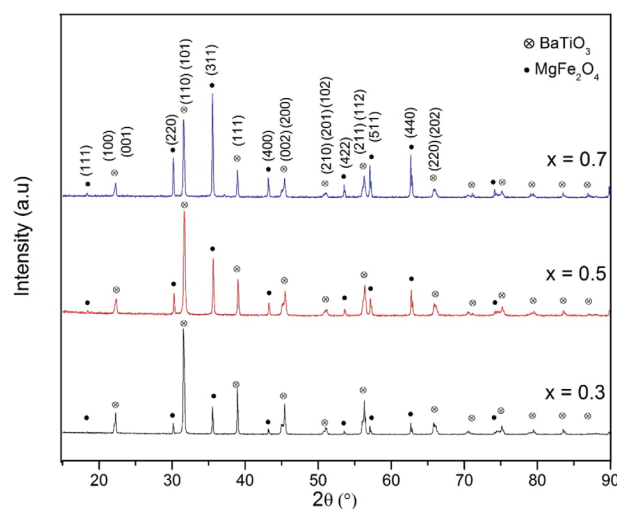


FIGURE 1. XRD patterns of  $(1-x)\text{BaTiO}_3$ - $x\text{MgFe}_2\text{O}_4$  composites with different weight fractions

XRD software that can be used to determine the percentage of two phases more precisely, which is shown in Table 1. From the table, there is only a slight differences between the theoretical and the experimental values of both phases confirming the absence of any impurities. A peak splitting at  $2\theta = 45^\circ$  suggest that there is a ferroelectric tetragonal phase with piezoelectric properties of Tadi et al. (2012). The average crystallite size and lattice parameters of  $\text{BaTiO}_3$  and  $\text{MgFe}_2\text{O}_4$  in the composite samples for each weight fraction were also calculated using *TOPAS* software and tabulated in Table 2. Composite sample with  $x = 0.5$  shows the smallest  $\text{BaTiO}_3$  and  $\text{MgFe}_2\text{O}_4$  crystallite size. Combination with  $\text{MgFe}_2\text{O}_4$  lowered the tetragonality ratio,  $c/a$  of  $\text{BaTiO}_3$ , which has a theoretical value of 1.011. (Leonel et al. 2011).

TABLE 1.  $\text{BaTiO}_3$  and  $\text{MgFe}_2\text{O}_4$  percentage measured using TOPAS

Weight fraction, x	Phase percentage (%)	
	$\text{BaTiO}_3$	$\text{MgFe}_2\text{O}_4$
0.3	69.97	30.03
0.5	49.45	50.55
0.7	29.83	70.17

Figure 2 illustrates the SEM micrographs of the cross section from the fractured surface of  $(1-x)\text{BaTiO}_3-x\text{MgFe}_2\text{O}_4$  composites pellets. It can be observed that grains with irregular shape and various sizes ranging from 0.1 to 1.2  $\mu\text{m}$  are evenly distributed across the samples with pores between the grains and formation of grains agglomeration. Sample with  $x = 0.5$  seems to have less pores compared to the other two composite sample. The average grain size was calculated using *ImageJ* software and was found that the average size of the grains are almost the same for all composite samples as shown in the Table 2. Although the weight fraction was changed, the grain size are not highly affected due to the same sintering temperature used for all samples.

Powdered sample was sandwiched between two circular tapes to form a very thin disk. It was put parallel to the applied external magnetic field and was analysed at room temperature. The  $M - H$  hysteresis loops for all samples were shown in Figure 3. The shape of the loops clearly shows a soft ferrimagnetic nature with low coercive field value. The magnetic behaviour is due to the presence of an ordered magnetic structure in the mixed spinel-perovskite system from the presence of  $\text{MgFe}_2\text{O}_4$  (Köferstein et al. 2015). The magnetization and coercive field of the samples were shown in Table 3. It is found that with the addition of  $\text{MgFe}_2\text{O}_4$  content, the values of

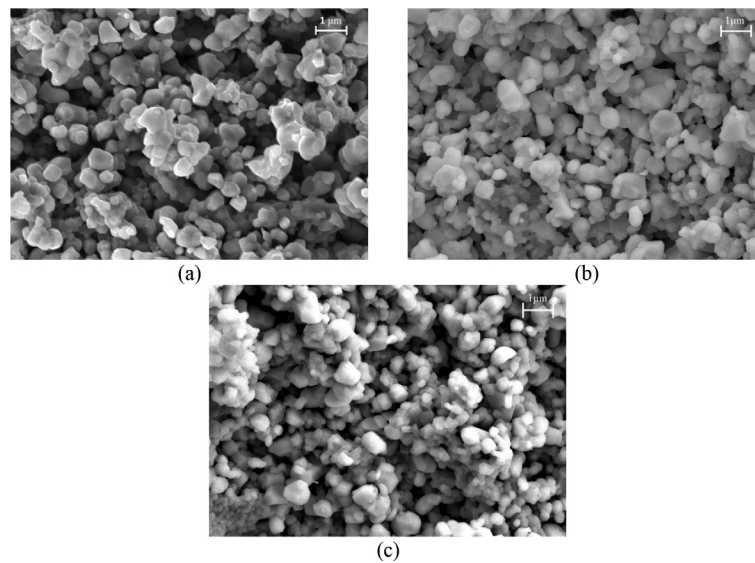


FIGURE 2. SEM images of  $(1-x)\text{BaTiO}_3-x\text{MgFe}_2\text{O}_4$  composites for (a)  $x = 0.3$ , (b)  $x = 0.5$  and (c)  $x = 0.7$

TABLE 2. Crystallite size, lattice parameters, tetragonality ratio of  $\text{BaTiO}_3$  and average grain size for each composite sample

Weight fraction, x	Crystallite size (nm)		Lattice parameter ( $\text{\AA}$ )			Tetragonality ratio of $\text{BaTiO}_3$ ( $c/a$ )	Average grain size ( $\mu\text{m}$ )
	$\text{BaTiO}_3$	$\text{MgFe}_2\text{O}_4$	$\text{BaTiO}_3$		$\text{MgFe}_2\text{O}_4$		
			$a = b$	$c$			
0.3	74	165	3.9957	4.0293	8.3820	1.0084	0.55 0.20
0.5	50	89	3.9990	4.0291	8.3858	1.0075	0.55 0.22
0.7	60	117	3.9982	4.0259	8.3837	1.0069	0.51 0.17

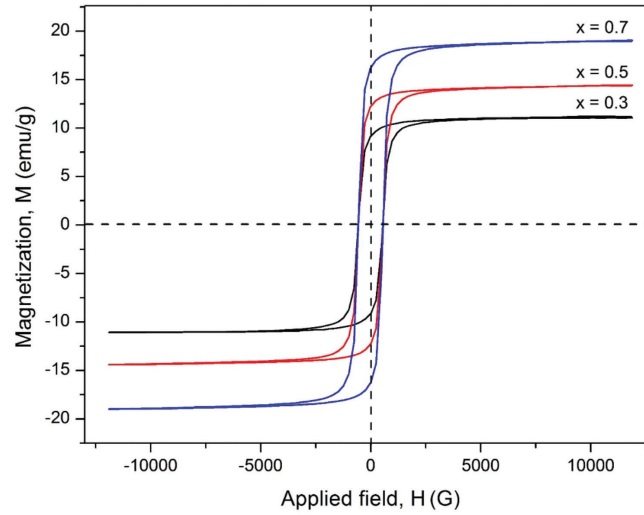


FIGURE 3. Magnetization,  $M$  versus magnetic field,  $H$  hysteresis loops for  $(1-x)$   $\text{BaTiO}_3$ - $x\text{MgFe}_2\text{O}_4$  composite with different weight fractions

TABLE 3. Magnetic parameters of each weight fractions of  $(1-x)\text{BaTiO}_3$ - $x\text{MgFe}_2\text{O}_4$

Weight fraction, $x$	Coercive field, $H_c$ (Oe)	Saturation magnetization, $M_s$ (emu/g)	Remanent magnetization, $M_r$ (emu/g)
0.3	54	11.1	9.2
0.5	55	14.3	12.5
0.7	56	19.1	16.2

saturation magnetization,  $M_s$  also increased. Magnetization of the samples was contributed by the ferrite grains in the composite which acts as a source of magnetic moments. By increasing the ferrite amount, it lead to a higher value of net magnetization due to the increasing of magnetic contacts between the ferrite grains (Hrib & Caltun 2011).  $\text{BaTiO}_3$ , as the ferroelectric material, integrated with  $\text{MgFe}_2\text{O}_4$  phase and affects the magnetic properties of the composites (Kanamadi et al. 2009). Remanent magnetization,  $M_r$  also increased with higher ferrite content. Due to the higher  $M_s$ , the magnetization left behind in the sample after an external magnetic field was removed is also high and the material remains magnetized (Callister 2007). Although  $\text{MgFe}_2\text{O}_4$  content increased the magnetization of the samples, the coercive field,  $H_c$  for the samples did not altered much because of the small variation of the grain size of the samples. The properties of magnetic coercive field was recognized through its microstructure such as density, magnetic phase percolation or ferrite doped with other ions. Coercive field was hard to control by using the variation of compositions (Mitoseriu & Buscaglia 2006).

The complex impedance spectroscopy is usually used to identify the AC electrical response contributed by the grain, grain boundary and the electrode with consideration of their different relaxation time. The Nyquist plot for all samples are shown in Figure 4 with a frequency range from 1 Hz to 10 MHz. Compressed single semicircle arc with the centre under the real impedance,  $Z'$  axis was obtained for all samples by using ZView software. The electrical process due to grain and grain boundary cannot be distinguished

clearly from the complex impedance loop. Therefore the equivalent circuit of the sample can be represented by a parallel bulk resistance,  $R$  and capacitance,  $C$  as shown in inlet of Figure 4. The bulk resistance value can be estimated from the intercept of the semicircular arc extension at  $Z'$  axis. The universal capacitor with a complex capacitance:

$$C^* = A(j\omega)^{n-1} = A\omega^n \left( \cos \frac{n\pi}{2} + j \sin \frac{n\pi}{2} \right),$$

is used to represent the ordinary capacitor due to the non-perfect semicircle where  $A$  is a constant, exponent  $n$  is the frequency dependence which is between 0 and 1 and  $\omega = 2\pi f_p = RC = 1$  with  $f_p$  is frequency at the peak of the impedance loop (Jonscher 1983). The complex impedance,  $Z^*$  data were fitted using:

$$Z^* = \frac{1}{Y^*}$$

$$Y^* = \frac{1}{R} \left[ 1 + \left( \frac{f}{f_p} \right)^n \cos \frac{n\pi}{2} \right] + \frac{j}{R} \left[ 1 + \left( \frac{f}{f_p} \right)^n \sin \frac{n\pi}{2} \right] \text{ with } 0 \leq n \leq 1.$$

Table 4 shows the parameters obtained from the fitting analysis. Composite sample with  $x = 0.5$  has the lowest value of capacitance,  $C$  and highest  $R$  compared to the others. Density, interface between ferrite and ferroelectric phase and oxygen vacancies are among the factors that influenced the variation in the resistance values (Pahuja et al. 2013). The peak frequency and  $n$  increased with higher  $\text{MgFe}_2\text{O}_4$  weight fraction.

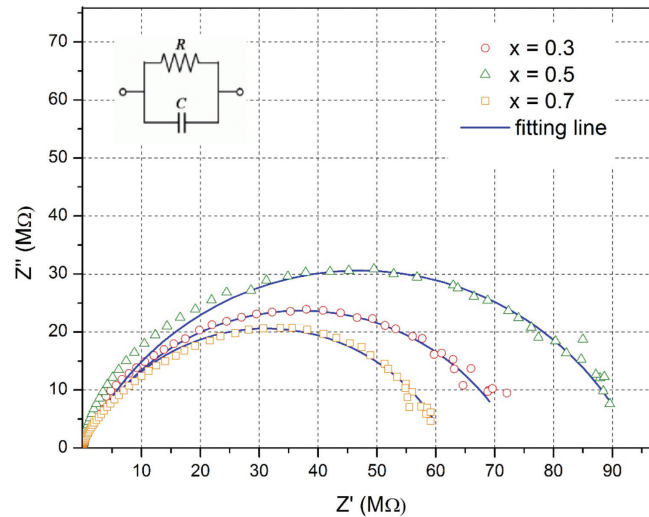


FIGURE 4. Complex impedance plots for all samples fitting lines and the equivalent  $R$ - $C$  circuit

TABLE 4. Capacitance, resistance, peak frequency and  $n$  for each composite

Weight fractions, $x$	Capacitance, $C$ (nF)	Resistance, $R$ (MΩ)	$n$	Peak frequency, $f_p$ (Hz)
0.3	0.114	73.0	0.735	15.8
0.5	0.081	93.0	0.740	21.0
0.7	0.136	62.0	0.743	22.5

Figure 5(a) shows the variation of dielectric constant with applied frequency measured at room temperature. A strongly dispersive region can be observed at low frequencies with a smaller dispersion at higher frequencies. The strong low frequency dispersion can be described by the Maxwell-Wagner relaxation mechanism (Pahuja et al. 2013). It may be a result of the interfacial or space charge polarization process between the  $\text{BaTiO}_3$  and  $\text{MgFe}_2\text{O}_4$  grains and between the material interface with the electrode. Factors that often contribute to the space charge polarization in materials is inhomogeneities in the dielectric structure such as impurities, porosity and grain structure (Mo et al. 2013). In dielectric-magnetic composite ceramics, there is a threshold of critical concentration and when this threshold state is achieved, the dielectric value increased significantly due to increasing of orientation polarization between ferrous ( $\text{Fe}^{2+}$ ) and ferric ( $\text{Fe}^{3+}$ ) ions in spinel ferrite (Zhang et al. 2013). At higher frequencies the dielectric constant is very low because charge carriers cannot follow the rapid change of the electric field direction (Pahuja et al. 2013).

As explained, dielectric constant depends on the applied frequency because there is a relaxation time for the charge transport. Composite sample with  $x = 0.07$  has the highest dielectric constant at lower frequency, followed by  $x = 0.03$  and 0.05. According to Liu et al. (2013), due to inhomogeneity between the two phases in the composite which is between  $\text{BaTiO}_3$  and  $\text{MgFe}_2\text{O}_4$ , there is a difference of the dielectric values at lower frequency (Liu et al. 2013). The ferroelectric phase was spread among

the spinel ferrite region in the composite. Based on Figure 5(b), high tangent loss were obtained for each composite and it decreased with increasing frequency. According to Köferstein et al. (2015), loss tangent increased with more  $\text{MgFe}_2\text{O}_4$  weight fraction in the composite due to the nature of  $\text{MgFe}_2\text{O}_4$  that has an electrically leakage properties (Köferstein et al. 2015). The leakage path to charge carrier was caused by the ferrite grains hence a conduction losses was increased. Therefore, there are a change in dielectric values and tangent loss when the  $\text{MgFe}_2\text{O}_4$  content was increased.

## CONCLUSION

$\text{MgFe}_2\text{O}_4$  powders were synthesized by the sol-gel autocombustion technique and successfully integrated with the commercial  $\text{BaTiO}_3$  powders to form  $(1-x)\text{BaTiO}_3$ - $x\text{MgFe}_2\text{O}_4$  multiferroics composite with different weight fractions,  $x = 0.3, 0.5$  and 0.7 by using wet milling solid state reaction method. The XRD patterns of the composites confirmed the formation of cubic spinel for  $\text{MgFe}_2\text{O}_4$  phase and tetragonal perovskite for  $\text{BaTiO}_3$  phases. The grain size of the composite samples does not change much with increment of weight fraction of  $\text{MgFe}_2\text{O}_4$ . The variation of ferrite content influenced the magnetic and the electrical properties of the composite. For magnetic characterization, all samples show the soft magnetic signal due to  $\text{MgFe}_2\text{O}_4$  presence and the composite with more  $\text{MgFe}_2\text{O}_4$  content has higher saturation and remanent magnetization which vary from 11.1 to 19.1 emu/g and 9.2

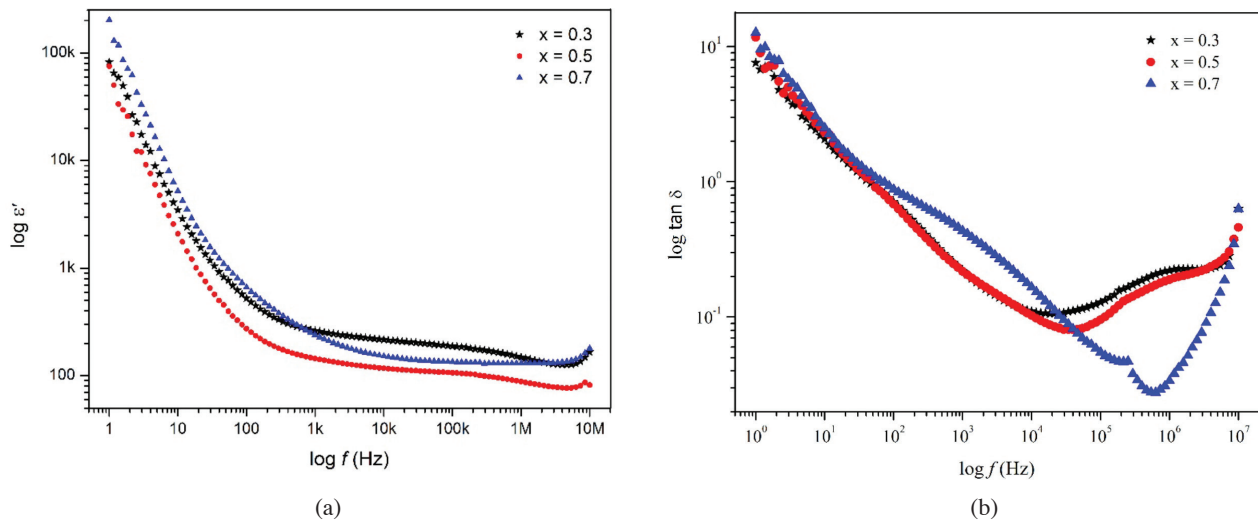


FIGURE 5. (a) Dielectric constant and (b) loss tangent of  $(1-x)\text{BaTiO}_3-x\text{MgFe}_2\text{O}_4$  multiferroics composite at different frequency

to 16.2 emu/g, respectively. However, the coercive field remains nearly the same. For the electrical properties, the semicircle arc impedance plot were fitted with a parallel R and  $C^*$  circuit and shows there are irregular trend in the resistance values of the composites due to variation of ferrite content. The sample of  $x = 0.5$  also has the lowest dielectric constant for the whole frequency range.

#### ACKNOWLEDGEMENTS

This research was supported by FRGS/2/2013/SG02/UKM/02/2 grant from the Malaysian Ministry of Higher Education. The author would like to thank the School of Applied Physics, Faculty of Science and Technology as well as Centre for Research and Instrumentation Mangement, Universiti Kebangsaan Malaysia for the facilities provided.

#### REFERENCES

- Callister, W.D. 2007. *Materials Science And Engineering: An Introduction*. New York: John Wiley & Sons.
- Fina, I., Dix, N., Fàbrega, L., Sánchez, F. & Fontcuberta, J. 2010. Magnetocapacitance in  $\text{BaTiO}_3\text{-CoFe}_2\text{O}_4$  nanocomposites. *Thin Solid Films* 518(16): 4634-4636.
- Hrib, L.M. & Caltun, O.F. 2011. Effects of the chemical composition of the magnetostrictive phase on the dielectric and magnetoelectric properties of cobalt ferrite-barium titanate composites. *Journal of Alloys and Compounds* 509(23): 6644-6648.
- Jonscher, A.K. 1983. *Dielectric Relaxation in Solids*. London: Chelsea Dielectrics Press Limited.
- Kanamadi, C.M., Kim, J.S., Yang, H.K., Moon, B.K., Choi, B.C. & Jeong, J.H. 2009. Magnetoelectric effect and complex impedance analysis of  $(x)\text{CoFe}_2\text{O}_4+(1-x)\text{Ba}_{0.8}\text{Sr}_{0.2}\text{TiO}_3$  multiferroics. *Journal of Alloys and Compounds* 481: 781-785.
- Köferstein, R., Walther, T., Hesse, D. & Ebbinghaus, S.G. 2015. Fine-grained  $\text{BaTiO}_3\text{-MgFe}_2\text{O}_4$  composites prepared by a Pechini-like process. *Journal of Alloys and Compounds* 638: 141-147.
- Leonel, L.V., Righi, A., Mussel, W.N., Silva, J.B. & Mohallem, N.D.S. 2011. Structural characterization of barium titanate-cobalt ferrite composite powders. *Ceramics International* 37(4): 1259-1264.
- Yu Lih-Jiun, Sahrim Hj Ahmad, Ing Kong, Sivanesan Appadu & Flaifel, M.H. 2012. Sifat magnet, mikrostruktur dan morfologi komposit getah asli termostplastik berpengisi Ferit NiZn/MwNT. *Sains Malaysiana* 41(4): 453-458.
- Liu, Y., Wu, Y., Li, D., Zhang, Y., Zhang, J. & Yang, J. 2013. A study of structural, ferroelectric, ferromagnetic, dielectric properties of  $\text{NiFe}_2\text{O}_4\text{-BaTiO}_3$  multiferroic composites. *Journal of Materials Science: Materials in Electronics* 24(6): 1900-1904.
- Mitoseriu, L. & Buscaglia, V. 2006. Intrinsic/extrinsic interplay contributions to the functional properties of ferroelectric-magnetic composites. *Phase Transitions* 79(12): 1095-1121.
- Mo, H.L., Jiang, D.M., Wang, C.M., Zhang, W.G. & Jiang, J.S. 2013. Magnetic, dielectric and magnetoelectric properties of  $\text{CoFe}_2\text{O}_4\text{-Bi}_{0.85}\text{La}_{0.15}\text{FeO}_3$  multiferroic composites. *Journal of Alloys and Compounds* 579: 187-191.
- Pahuja, P., Sharma, R., Prakash, C. & Tandon, R.P. 2013. Synthesis and characterization of  $\text{Ni}_{0.8}\text{Co}_{0.2}\text{Fe}_2\text{O}_4\text{-Ba}_{0.95}\text{Sr}_{0.05}\text{TiO}_3$  multiferroic composites. *Ceramic International* 39: 9435-9445.
- Ravindar Tadi, Yong-Il Kim, Debasish Sarkar, Cheolgi Kim & Ryu, K.S. 2010. Magnetic and electrical properties of bulk  $\text{BaTiO}_3 + \text{MgFe}_2\text{O}_4$  composite. *Magnetism and Magnetic Materials* 323: 564-658.
- Roy, A., Gupta, R. & Garg, A. 2012. Review article: Multiferroic memories. *Advances in Condensed Matter Physics* 2012: 12.
- Siong, K.K., Amari, N.F., Yuan, T.C., Radiman, S., Yahaya, R. & Yasir, M.S. 2013. Preparation, characterization and properties of core-shell cobalt ferrite/polycaprolactone nanomagnetic biomaterials. *Sains Malaysiana* 42(2): 167-173.
- Spaldin, N., Cheong, S. & Ramesh, R. 2010. Multiferroics: Past, present, and future. *Physics Today* 63(10): 38-43.
- Sutka, A. & Mezinskis, G. 2012. Sol-gel auto-combustion synthesis of spinel-type ferrite nanomaterials. *Frontiers of Materials Science* 6(2): 128-141.
- Tadi, R., Kim, Y.I., Ryu, K.S. & Kim, C. 2012. Effect of magnetic field on the dielectric properties of multiferroic composites. *Journal of the Korean Physical Society* 61(9): 1545-1549.

- Yadav, R.S., Havlica, J., Masilko, J., Kalina, L., Wasserbauer, J., Hajdúchová, M., Enev, V., Kuřitka, I. & Kožáková, Z. 2016. Impact of  $\text{Nd}^{3+}$  in  $\text{CoFe}_2\text{O}_4$  spinel ferrite nanoparticles on cation distribution, structural and magnetic properties. *Journal of Magnetism and Magnetic Materials* 399: 109-117.
- Zhang, R.F., Deng, C.Y., Ren, L., Li, Z. & Zhou, J.P. 2013. Dielectric, ferromagnetic and magnetoelectric properties of  $\text{BaTiO}_3\text{-Ni}_{0.7}\text{Zn}_{0.3}\text{Fe}_2\text{O}_4$  composite ceramics. *Materials Research Bulletin* 48(10): 4100-4104.
- Zolkepli, M.F.A. & Zainuddin, Z. 2015. Structure, magnetic and complex impedance analysis of  $(1-x)\text{BaTiO}_3\text{-xMgFe}_2\text{O}_4$  composite. *AIP Conference Proceedings* 1678: 040014.

Pusat Pengajian Fizik Gunaan  
Fakulti Sains dan Teknologi  
Universiti Kebangsaan Malaysia  
43600 UKM Bangi, Selangor Darul Ehsan  
Malaysia

\*Corresponding author; email: zazai@ukm.edu.my

Received: 11 April 2016

Accepted: 25 November 2016